

A COMPREHENSIVE ANALYSIS OF MULTI-LEVEL INVERTERS IN SINGLE-PHASE PHOTOVOLTAIC SYSTEMS

Venkatesh Tadivalasa¹, Relli Pavani², R.Triveni³, G.Divya⁴, K.Mohan⁵, S.Venkatarao⁶

^{1,2}Assistant Professor, Department of Electrical and Electronics Engineering, Satya Institute of Technology and Management, Vizianagaram, Andhra Pradesh, India

^{3,4,5,6}B.tech Student, Department of Electrical and Electronics Engineering, Satya Institute of Technology and Management, Vizianagaram, Andhra Pradesh, India

Email: trivenirukana69@gmail.com¹

Abstract - This paper explores single-phase grid-connected inverters for small-scale applications, typically below 10 kW. It introduces a novel solution: a single-phase seven-level inverter for grid-connected photovoltaic systems. Unlike traditional three-level inverters, this design aims to mitigate issues like increased switching losses and interference. It employs a unique PWM control scheme utilizing three identical reference signals offset to the triangular carrier signal's amplitude, generating seven output voltage levels from the DC supply. MATLAB analysis demonstrates the inverter's behavior, showing its ability to achieve the desired voltage levels through modulation index control. A comparison with an 11-level inverter design underscores the effectiveness of the proposed seven-level inverter in improving output waveforms and reducing total harmonic distortion.

Key Words: PV System, MPPT, Boost Chopper, 11-level Inverter.

1.INTRODUCTION

The escalating global energy demand, coupled with the rising costs and finite nature of fossil fuels, alongside environmental concerns, has spurred a significant interest in renewable energy sources. Photovoltaic (PV) systems represent a prominent solution, harnessing the Sun's energy directly to generate electricity. These systems rely on grid-connected inverters to deliver the generated energy to power networks. In particular, single-phase grid-connected inverters find application in residential or low-power settings, typically below 10 kW.

Single-phase grid-connected inverters play a vital role in converting direct current (DC) from renewable energy sources like photovoltaic systems into alternating current (AC) for residential and low-power applications. While the full-bridge three-level topology is widely used for its high switching capabilities, it suffers from drawbacks such as increased switching losses, acoustic noise, and interference with other equipment. Addressing these issues is essential

for improving overall performance and reducing operational drawbacks.

Multilevel inverters have emerged as a promising solution due to their ability to produce nearly sinusoidal output-voltage waveforms, improved harmonic profiles in output current, reduced stress on electronic components, lower switching losses compared to conventional two-level inverters, and smaller filter requirements resulting in lower electromagnetic interference (EMI). These advantages contribute to cost-effectiveness, lighter weight, and compactness of the inverters.

Various topologies for multilevel inverters have been proposed over the years, including diode-clamped, flying capacitor or multicell, cascaded H-bridge, and modified H-bridge multilevel inverters. Among these, the modified H-bridge single-phase multilevel inverter stands out for its potential to address the limitations of traditional full-bridge inverters effectively.

This paper focuses on the development of a novel modified H-bridge single-phase multilevel inverter. The design incorporates two diode-embedded bidirectional switches and a unique pulse width modulation (PWM) technique. By utilizing these components and techniques, the proposed inverter aims to mitigate the drawbacks associated with conventional full-bridge inverters while leveraging the benefits of multilevel topology. Specifically, the integration of diode-embedded bidirectional switches enhances switching efficiency and reduces losses, while the novel PWM technique ensures improved waveform quality and reduced EMI.

The proposed topology is implemented in a grid-connected photovoltaic system, incorporating both a maximum power point tracker (MPPT) and a current control algorithm. The MPPT ensures the system operates at its maximum power output by continuously tracking and adjusting for variations

in solar irradiance and temperature. The simulated results obtained with MPPT implementation are thoroughly explained, highlighting the effectiveness of the proposed approach in optimizing power generation from the photovoltaic system while mitigating operational drawbacks associated with conventional inverters.

2. PHOTOVOLTAIC SYSTEM

2.1 Photovoltaic Effect

Photovoltaic (PV) technology harnesses solar radiation by converting it into direct current electricity through the photovoltaic effect exhibited by semiconductors.

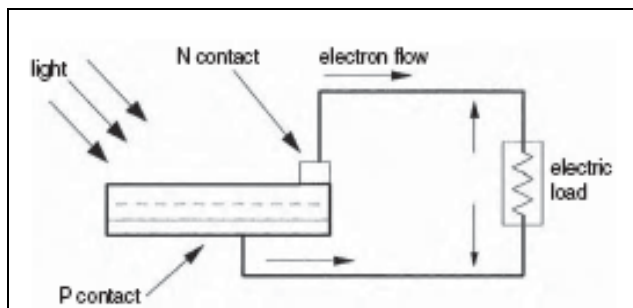


Fig 2.1: PV effect converts the photon energy into voltage across the p-n junction

Solar panels for photovoltaic power generation consist of cells made from a variety of photovoltaic materials, including mono-crystalline silicon, polycrystalline silicon, amorphous silicon, cadmium telluride, and copper indium selenide/sulfide. Recent progress in solar cell and photovoltaic array production has been fueled by the growing need for renewable energy sources.

2.2 Equivalent Circuit

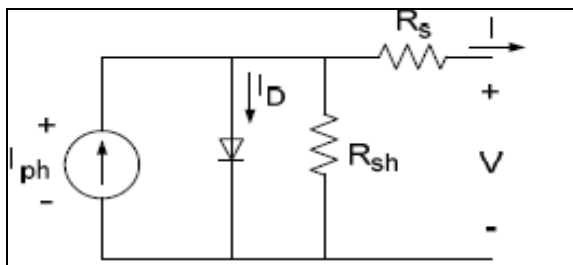


Fig 2.2 PV cell equivalent circuit

The behavior of photovoltaic (PV) cells can be accurately represented by an equivalent electrical circuit, which includes several crucial parameters. Series resistance (R_s) reflects the internal resistance hindering current flow within the cell, influenced by factors such as pn-junction depth, impurities, and contact resistance. Conversely, shunt resistance (R_{sh}) is inversely proportional to the leakage

current to ground. In an ideal scenario, R_s would be 0 ohms, indicating no series loss, while R_{sh} would be infinite, suggesting no leakage to ground. However, in high-quality silicon cells, R_s typically falls within the range of 0.05 to 0.10 ohms, whereas R_{sh} ranges from 200 to 300 ohms.

PV conversion efficiency is highly sensitive to even minor variations in R_s but remains largely unaffected by changes in R_{sh} . Even a slight increase in R_s can significantly reduce PV output. In the equivalent circuit, the current supplied to the external load equals the generated illumination current (I_{ph}), minus the diode current (I_D) and shunt leakage current (I_{sh}). The open-circuit voltage (V_{oc}) of the cell is determined when the load current is zero ($I = 0$).

Essentially, understanding and controlling these circuit parameters are crucial for optimizing PV cell performance and overall system efficiency. Accurate characterization and management of R_s and R_{sh} enable precise modeling and prediction of PV cell behavior under various operating conditions, ultimately facilitating the design and optimization of photovoltaic systems for maximum energy harvest.

$$V_{oc} = V + IR_{sh}$$

Shunt resistance (R_{sh}) in photovoltaic cells is typically large, while series resistance (R_s) is very small. Consequently, it is a common practice to disregard these resistances for the sake of simplifying the solar cell model. This simplification leads to an ideal voltage-current characteristic, as depicted in the accompanying figure.

$$I = I_{ph} - I_D$$

$$I = I_{ph} - I_0$$

2.3 Maximum Power Point Tracking

Maximum power point

The operating point A, labeled as (V_{max} , I_{max}), signifies the point where the power dissipated in the resistive load reaches its peak.

Maximum efficiency

The ratio between the maximum power and the incident light power is a critical metric in evaluating the performance of photovoltaic (PV) devices. Typically, module characteristics provided by manufacturers are determined under specific conditions, often involving known irradiance levels.

The operating point A, characterized by (V_{max} , I_{max}), represents the configuration where the power dissipated in

the resistive load achieves its peak value, calculated as $P_{max} = I_{max} * V_{max}$. This point is crucial for Maximum Power Point Tracking (MPPT), which aims to optimize power collection. The maximum irradiance value for MPPT is typically set at 1000 W/m^2 , ensuring that the system captures the highest available power.

Leveraging MPPT techniques enhances the efficiency and output response of PV cells. By continuously adjusting the operating point to match the maximum power available under varying environmental conditions, MPPT maximizes energy harvest and improves the overall performance of PV systems. This approach ensures that the PV device operates at its peak efficiency, thereby maximizing its power output and contributing to enhanced renewable energy utilization.

2.3.1 MPPT Algorithms

Maximum Power Point Trackers (MPPT) employ diverse algorithms that dynamically adjust the operating point of photovoltaic arrays to maximize power output under varying conditions. Common MPPT algorithms include:

Constant Voltage: This method maintains a constant voltage across the PV array, adjusting the current to maximize power output.

Short Circuit Current: By keeping the load impedance at zero (short circuit condition), this algorithm seeks to maximize current flow and consequently power output.

Incremental Conductance: This algorithm continuously monitors the array's conductance and adjusts the operating point to match the point where the conductance equals the negative ratio of the array's voltage to its current.

Perturb and Observe: Termed as the hill-climbing method, this algorithm systematically perturbs the operating point, monitoring the consequent change in power output, and adjusts the operating point towards maximizing power output.

Each algorithm has its advantages and drawbacks, and the choice depends on factors such as system complexity, efficiency, and response time. Additionally, MPPT systems may switch between algorithms based on real-time operating conditions to ensure optimal performance under varying environmental factors.

2.3.2 Proposed MPPT Algorithm

The proposed MPPT algorithm utilizes the Perturb and Observe method with current control. Designers typically have the option to adjust either the photovoltaic (PV) voltage or current to optimize power output. Figure 2.3

illustrates the relationship between changes in the Maximum Power Voltage (V_{MP}) and the natural logarithm of irradiance ($\ln(\text{irradiance})$). This indicates that V_{MP} varies closely with irradiance levels. Additionally, Figure 2.4 demonstrates that the Maximum Power Current (I_{MP}) is directly proportional to irradiance, highlighting the impact of irradiance variations on current levels.

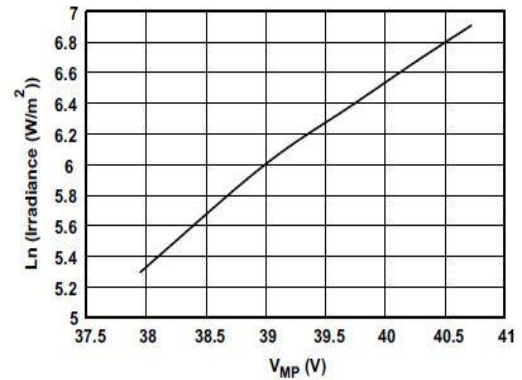


Figure 2.3 Irradiance vs V_{MP} for 200 to 1000 W/m^2

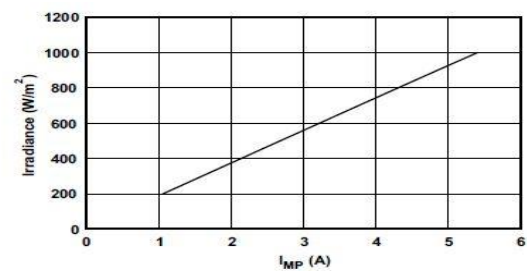


Figure 2.4 Irradiance vs I_{MP} for 200 to 1000 W/m^2

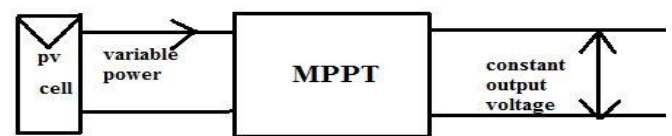


Fig 2.5 Block diagram of P&O Algorithm

3. STEP-UP CHOPPER/ BOOST CHOPPER

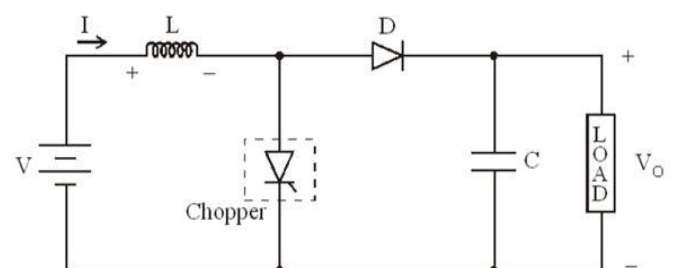


Fig 3.1 Step-Up Chopper/Boost Chopper

Figure 3.1 illustrates a step-up chopper designed to attain a load voltage (V_o) higher than the input voltage (V). The determination of inductor (L) and capacitor (C) values depends on the precise needs for output voltage and current. In the ON state of the chopper, when it actively conducts, inductor L is linked across the power supply. This operational phase, denoted as T_{on} , facilitates the rise of inductor current ' I ,' allowing the inductor to accumulate and store energy.

Upon switching off the chopper, the inductor current ' I ' is redirected to pass through the diode (D) and the load for a period labeled T_{off} . During this OFF state, the inductor current tends to decrease, causing a reversal in the polarity of the induced electromotive force (EMF) within the inductor (L). This cyclical process of energy storage during the chopper's ON state and its subsequent release during the OFF state enables the step-up chopper to effectively elevate the load voltage, achieving the desired output levels. The careful selection of inductor and capacitor values ensures optimal performance in accordance with the specified output voltage and current requirements.

The thyristor in the circuit acts as a crucial switch. In its conducting state (ON), the supply voltage appears across the load. Conversely, when the thyristor is non-conducting (OFF), the voltage across the load drops to zero. The depicted circuit embodies a step-up or Pulse Width Modulated (PWM) boost converter configuration. It consists of a DC input voltage source (V_S), a boost inductor (L), a controlled switch (S), a diode (D), a filter capacitor (C), and a load resistance (R).

In Continuous Conduction Mode (CCM), the converter waveforms depicted in the accompanying figure illustrate the operational phases. During the ON state of switch S , the current within the boost inductor increases linearly, while diode D remains non-conductive. Subsequently, when switch S transitions to its OFF state, the energy stored within the inductor is discharged through the diode, supplying power to the designated load (R -Load).

This cyclic process of energy storage and release, facilitated by the ON/OFF states of the switch and diode, respectively, defines the operation of the step-up or PWM boost converter. It enables the conversion of input DC voltage to a higher output voltage level, thus fulfilling the intended function of the converter within the electrical circuit.

4. INVERTERS

4.1 Introduction to Inverters

Direct Current to Alternating Current (D.C.-A.C.) inverters serve as electronic devices designed to transform low-voltage D.C. energy, sourced from batteries or solar panels,

into mains voltage A.C. power. This functionality proves invaluable in situations where traditional A.C. mains power is unavailable, such as in caravans, mobile homes, or remote areas requiring the operation of audio, video, and computing equipment. The core operations of most inverters involve two primary functions: firstly, the conversion of incoming D.C. into A.C., and secondly, the elevation of the resulting A.C. to mains voltage levels, accomplished through the utilization of a transformer.

Efficiency is a paramount consideration for designers, aiming to optimize the inverter's performance. The objective is to ensure that the conversion process is as efficient as possible, maximizing the transformation of energy drawn from the battery or solar panel into mains voltage A.C., while minimizing energy wastage in the form of heat. This efficiency-driven design approach enhances the overall utility and sustainability of D.C.-A.C. inverters in diverse applications.

4.2 Proposed Multilevel Inverter Topology

The proposed single-phase seven-level inverter evolved from a five-level inverter design, comprising essential components such as a single-phase conventional H-bridge inverter, two bidirectional switches, and a capacitor voltage divider formed by C_1 , C_2 , and C_3 . This modified H-bridge topology offers significant advantages over alternative configurations, including reduced power switch and diode requirements, as well as a decreased number of capacitors, all while maintaining the same number of output levels.

The integration of photovoltaic (PV) arrays into the system necessitated the inclusion of a DC-DC boost converter to bridge the voltage gap between the PV array and the utility grid. Since PV arrays typically operate at lower voltages compared to the grid, the boost converter facilitates the generation of high DC bus voltages essential for enabling power flow from the PV arrays to the grid.

To ensure smooth power delivery to the grid, a filtering inductance (L_f) was introduced to filter the current injected into the grid, enhancing grid stability and reducing harmonic distortions.

The operation of the proposed inverter involves seven distinct switching states, each facilitating the generation of specific output-voltage levels (V_{dc} , $2V_{dc}/3$, $V_{dc}/3$, 0 , $-V_{dc}$, $-2V_{dc}/3$, $-V_{dc}/3$) from the DC supply voltage. These switching states, illustrated in Figures 4.1 through 4.7, define the inverter's operational behavior and facilitate the production of various output voltage levels to meet the requirements of the grid-connected power network.

Overall, the proposed single-phase seven-level inverter represents an innovative solution that leverages modified H-

bridge topology and advanced switching techniques to enable efficient power conversion and integration of PV arrays into the utility grid, contributing to enhanced grid stability and renewable energy utilization.

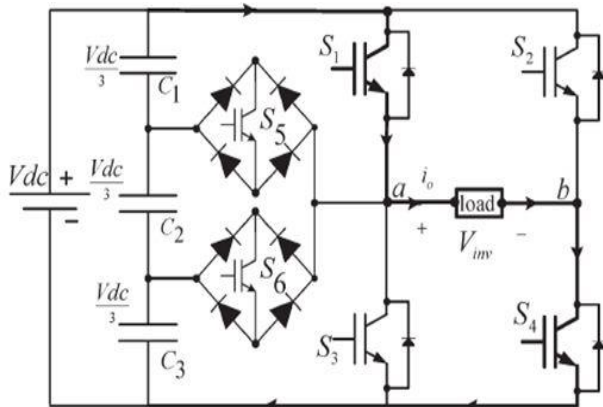


Fig 4.1 Inverter circuit for the output voltage (V_{dc})

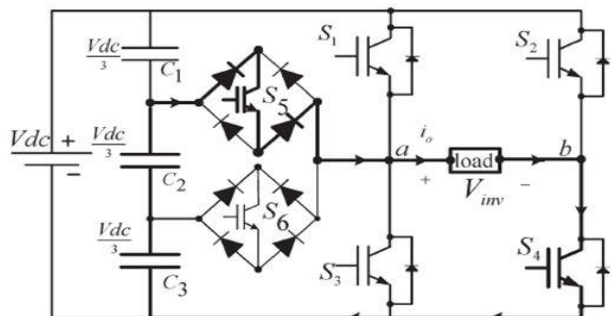


Fig 4.2 Inverter circuit for the output voltage ($2V_{dc}/3$)

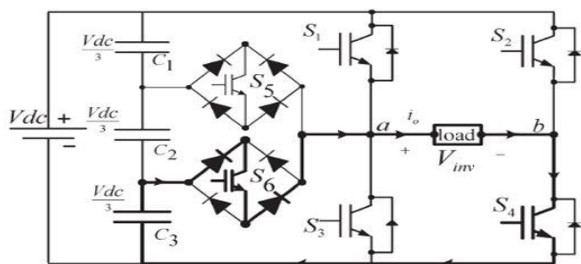


Fig 4.3 Inverter circuit for the output voltage ($V_{dc}/3$)

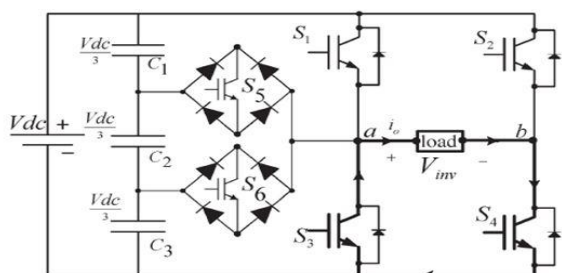


Fig 4.4 Inverter circuit for the output voltage (zero 0)

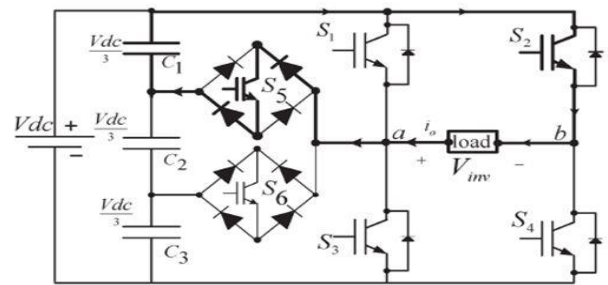


Fig 4.5 Inverter circuit for the output voltage ($-V_{dc}/3$)

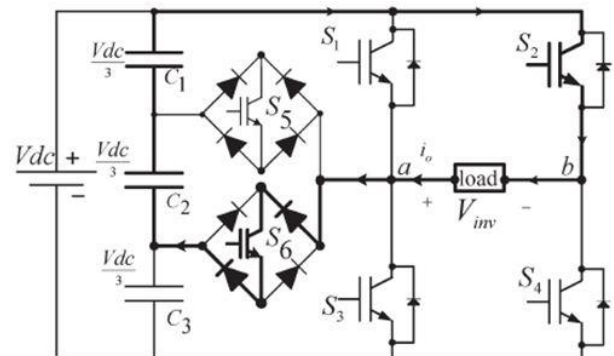


Fig 4.6 Inverter circuit for the output voltage ($-2V_{dc}/3$)

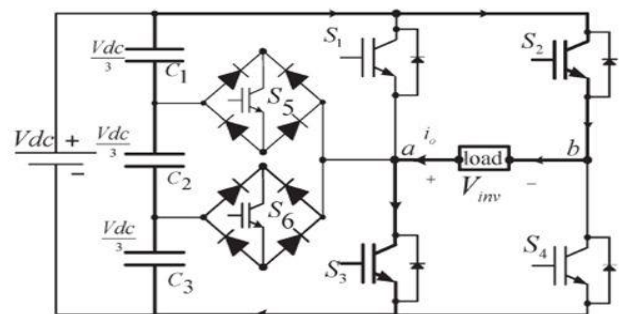


Fig 4.7 Inverter circuit for the output voltage ($-V_{dc}$)

Table 4.1 Output voltage according to the switches on-off condition

v_0	S_1	S_2	S_3	S_4	S_5	S_6
V_{dc}	on	off	off	on	off	off
$2V_{dc}/3$	off	off	off	on	on	off
$V_{dc}/3$	off	off	off	on	off	on
0	off	off	on	on	off	off
0*	on	on	off	off	off	off
$-V_{dc}/3$	off	on	off	off	on	off
$-2V_{dc}/3$	off	on	off	off	off	on
$-V_{dc}$	off	on	on	off	off	off

The table outlines the specific switching combinations responsible for generating the seven distinct output-voltage levels (0, $-V_{dc}$, $-2V_{dc}/3$, $-V_{dc}/3$, V_{dc} , $2V_{dc}/3$, $V_{dc}/3$). Each entry in the table corresponds to a unique configuration of the switches, capturing the precise arrangement required to achieve the desired output voltage level. This

comprehensive mapping of switching combinations provides a clear reference for understanding and controlling the inverter's operation, ensuring the accurate generation of the specified output voltage levels based on the applied DC supply voltage (Vdc). The table serves as a valuable tool for engineers and practitioners involved in the design, analysis, and optimization of the single-phase seven-level inverter, facilitating a systematic approach to its operation and performance.

5. CONTROL STRATEGY

5.1 Introduction

As shown in Figure 5.1, the control system of the proposed inverter consists of various components, including a Maximum Power Point Tracking (MPPT) algorithm, a DC-bus voltage controller, reference-current generation, and a current controller. This control system has dual objectives: maximizing energy transfer from the PV arrays to the grid and generating a sinusoidal current with minimal harmonic distortion, even in the presence of grid voltage harmonics.

The perturb-and-observe (P&O) algorithm is selected for Maximum Power Point Tracking (MPPT) due to its simplicity and minimal requirement of measured parameters. This algorithm periodically adjusts the array terminal voltage and compares the PV output power with that of the previous cycle, fine-tuning the voltage accordingly. Implemented in the DC-DC boost converter, the P&O algorithm ensures efficient energy transfer from the PV arrays.

The output of the MPPT algorithm is a duty-cycle function, modulating the voltage at the PV panels' output via the AC-DC seven-level PWM inverter. A Proportional-Integral-Derivative (PID) controller maintains a constant output voltage (Vdc) of the DC-DC boost converter by comparing Vdc with a reference voltage (Vdcref) and adjusting the duty cycle accordingly.

For grid synchronization, a method is necessary to align the inverter output with the grid. This involves detecting the grid period and phase to ensure frequency and phase match between the PV inverter and the grid. A sine lookup table generates reference current aligned with the grid voltage (Vload). PID controllers generate the sinusoidal signal, while a sine lookup table and zero-crossing detector assist in achieving synchronization.

Overall, the control system operates under closed-loop conditions to ensure accurate and efficient energy transfer from the PV arrays to the grid, while maintaining grid synchronization and minimizing harmonic distortion in the output current.

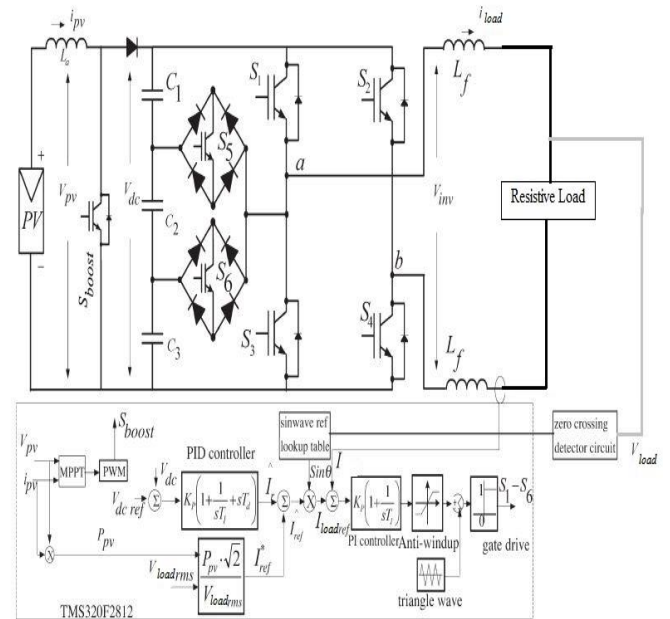


Fig. 5.1 Seven-level inverter with closed-loop control algorithm

6. SIMULATION RESULTS

6.1 Block Diagrams

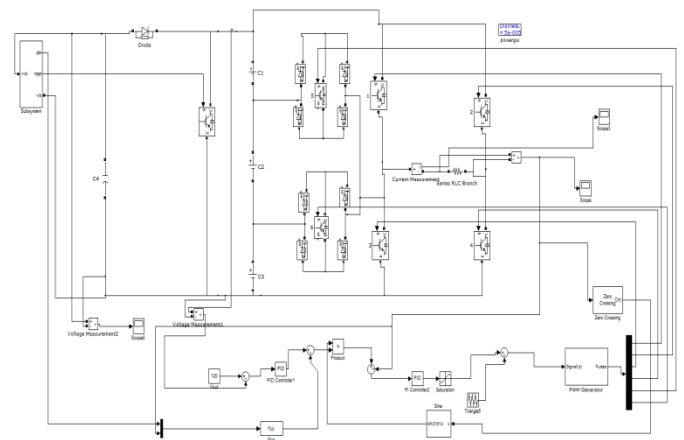


Fig. 6.1 Main MATLAB/Simulink Seven level Inverter Block diagram

6.2 Simulation Results

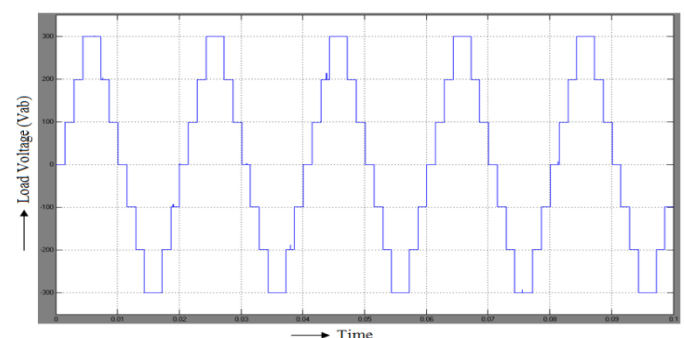


Fig 6.2 Seven levels of Inverter output voltage (V_{inv})

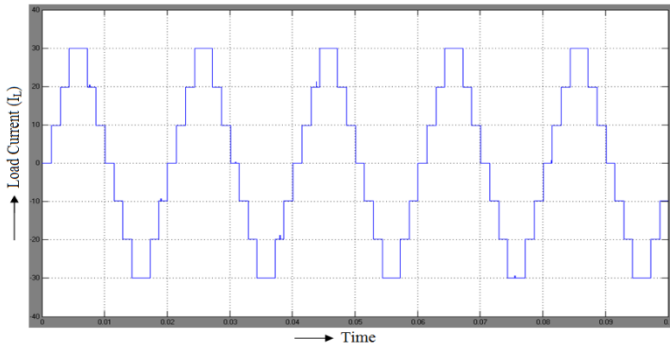


Fig 6.3 Seven levels of Inverter output current (I_{inv})

For $R=10\Omega$

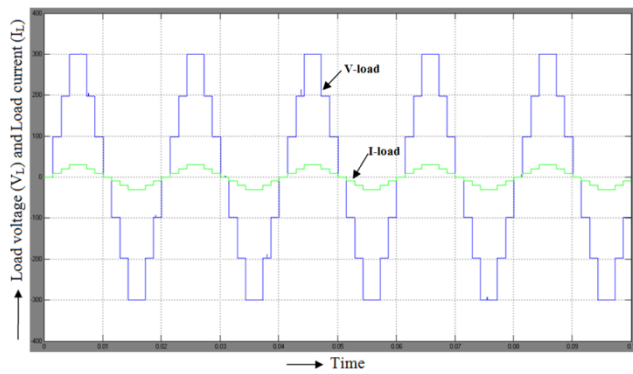


Fig 6.4 Load voltage (V_{Load}) and Load current (I_{Load}) that are in phase

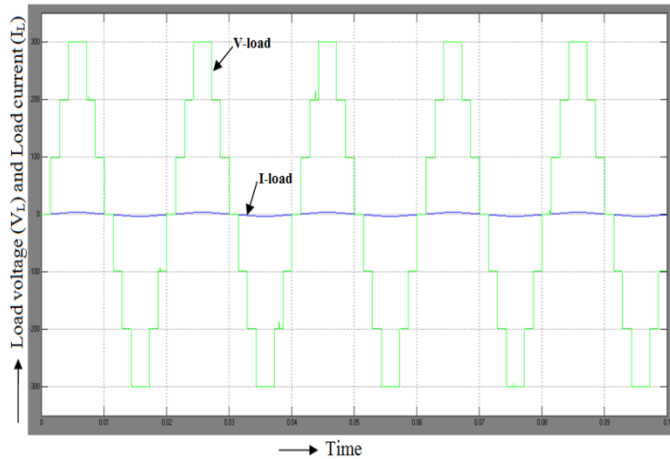


Fig 6.5 Load voltage (V_{Load}) and Load current (I_{Load}) that are in phase

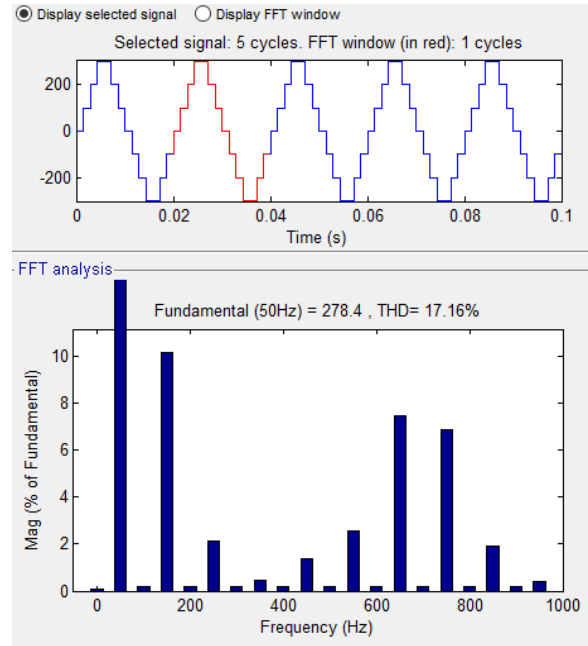


Fig. 6.6. THD for seven level inverter

6.3 Eleven Level Inverter

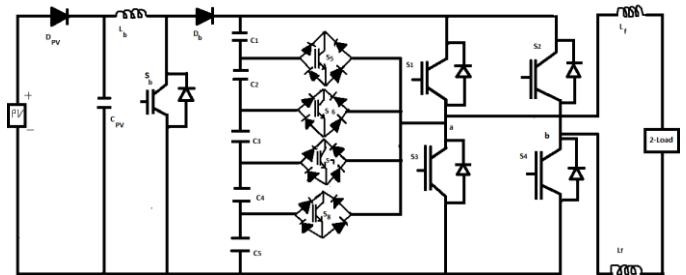


Fig 6.7 Main MATLAB/Simulink Eleven level Inverter Block diagram

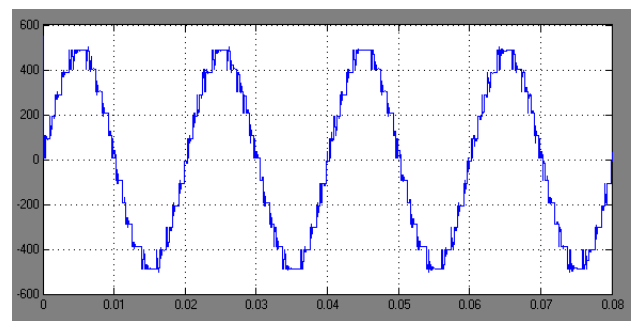


Fig 6.8 Eleven levels of Inverter output voltage (V_{inv})

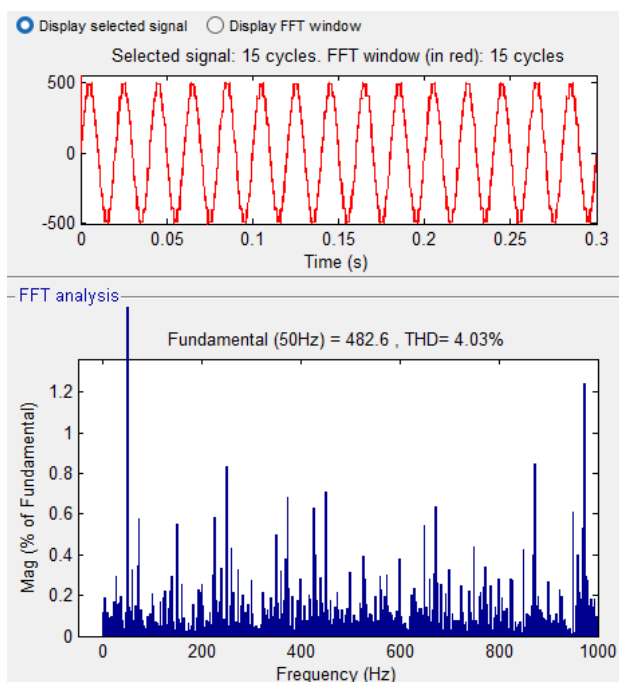


Fig. 6.9. THD for Eleven level inverter

7. CONCLUSIONS

This paper introduces a novel Pulse Width Modulation (PWM) switching scheme tailored for the proposed multilevel inverter, presenting a distinct method for generating voltage output. By integrating three reference signals and a triangular carrier signal, this scheme efficiently produces PWM switching signals, ensuring precise control over the inverter's output voltage levels. Thorough analysis delves into the behavior of the proposed multilevel inverter, scrutinizing its performance under varied operating conditions.

A significant advantage of this PWM scheme lies in its modulation index control capability, facilitating the attainment of the desired number of output voltage levels in the inverter. This adaptability enables customization of the inverter's performance to suit specific application needs. Notably, the achieved reduction in Total Harmonic Distortion (THD) in the seven-level inverter presents an attractive solution for grid-connected Photovoltaic (PV) inverters. The diminished THD contributes to enhanced overall system response and efficiency.

Comparative analysis with an eleven-level inverter further accentuates the benefits of the proposed seven-level inverter. While the eleven-level inverter exhibits reduced THD, the seven-level inverter offers comparable performance with fewer switching states, enhancing reliability and simplifying operation. This balance between THD reduction and complexity underscores the practical viability of the seven-level inverter for grid-connected PV applications.

In summary, the proposed PWM switching scheme presents a promising solution for multilevel inverters, offering precise control over output voltage levels and facilitating improved system response. While the seven-level inverter demonstrates less THD compared to its eleven-level counterpart, it achieves this with fewer switching states, ensuring reliable and efficient operation in grid-connected PV systems.

REFERENCES

- [1] Nasrudin A. Rahim, Jeyraj Selvaraj, "Single-Phase Seven-Level Grid-Connected Inverter for Photovoltaic System", *IEEE Trns. on industrial electronics*, VOL. 58, NO. 6, JUNE 2011.
- [2] S. B. Kjaer, J. K. Pedersen, and F. Blaabjerg, "A review of single-phase grid connected inverters for photovoltaic modules," *IEEE Trans. Ind. Appl.*, vol. 41, no. 5, pp. 1292–1306, Sep./Oct. 2005.
- [3] J. Rodríguez, J. S. Lai, and F. Z. Peng, "Multilevel inverters: A survey of topologies, controls, and applications," *IEEE Trans. Ind. Electron.*, vol. 49, no. 4, pp. 724–738, Aug. 2002.
- [4] J. Selvaraj and N. A. Rahim, "Multilevel inverter for grid-connected PV system employing digital PI controller," *IEEE Trans. Ind. Electron.*, vol. 56, no. 1, pp. 149–158, Jan. 2009.
- [5] Dinesh, L., Sesham, H., & Manoj, V. (2012, December). Simulation of D-Statcom with hysteresis current controller for harmonic reduction. In *2012 International Conference on Emerging Trends in Electrical Engineering and Energy Management (ICETEEEM)* (pp. 104-108). IEEE
- [6] J. Huang and K. A. Corzine, "Extended operation of flying capacitor multilevel inverter," *IEEE Trans. Power Electron.*, vol. 21, no. 1, pp. 140–147, Jan. 2006.
- [7] Manoj, V. (2016). Sensorless Control of Induction Motor Based on Model Reference Adaptive System (MRAS). *International Journal For Research In Electronics & Electrical Engineering*, 2(5), 01-06.
- [8] J. I. Leon, S. Vazquez, S. Kouro, L. G. Franquelo, J. M. Carrasco, and J. Rodriguez, "Unidimensional modulation technique for cascaded multilevel converters," *IEEE Trans. Ind. Electron.*, vol. 49, no. 5, pp. 1058–1064, Oct. 2002.
- [9] V. B. Venkateswaran and V. Manoj, "State estimation of power system containing FACTS Controller and PMU," 2015 IEEE 9th International Conference on Intelligent Systems and Control (ISCO), 2015, pp. 1-6, doi: 10.1109/ISCO.2015.7282281.
- [10] Manohar, K., Durga, B., Manoj, V., & Chaitanya, D. K. (2011). Design Of Fuzzy Logic Controller In

DC Link To Reduce Switching Losses In VSC Using MATLAB-SIMULINK. *Journal Of Research in Recent Trends*.

- [11] Manoj, V., Manohar, K., & Prasad, B. D. (2012). Reduction of switching losses in VSC using DC link fuzzy logic controller *Innovative Systems Design and Engineering ISSN, 2222-1727*.
- [12] G. Ceglia, V. Guzman, C. Sanchez, F. Ibanez, J. Walter, and M. I. Gimanez, "A new simplified multilevel inverter topology for DC-AC conversion," *IEEE Trans. Power Electron.*, vol. 21, no. 5, pp. 1311–1319, Sep. 2006.
- [13] N. A. Rahim and J. Selvaraj, "Multi-string five-level inverter with novel PWM control scheme for PV application," *IEEE Trans. Ind. Electron.*, vol. 57, no. 6, pp.2111–2121, Jun. 2010.
- [14] Dinesh, L., Harish, S., & Manoj, V. (2015). Simulation of UPQC-IG with adaptive neuro fuzzy controller (ANFIS) for power quality improvement. *Int J Electr Eng, 10, 249-268*.
- [15] E. Villanueva, P. Correa, J. Rodríguez, and M. Pacas, "Control of a single phase cascaded H-bridge multilevel inverter for grid-connected photovoltaic systems," *IEEE Trans. Ind. Electron.*, vol. 56, no. 11, pp. 4399–4406, Nov. 2009.
- [16] "Modeling and Simulation of Photovoltaic module using MATLAB/Simulink", *International Journal of Chemical and Environmental Engineering*, Volume 2, No.5 , October 2011.
- [17] "Mathematical Modeling and Simulation of Photovoltaic Cell using Matlab-Simulink Environment", *International Journal of Electrical and Computer Engineering (IJECE)*, Vol. 2, No. 1, February 2012